Development of Lattice-Mismatched GaInAsP for Radiation Hardness

Ryan M. France, Pilar Espinet-Gonzalez, Brian B. Haidet, Kunal Mukherjee, Harvey L. Guthrey, Harry A. Atwater, and Don Walker

***Abstract*—We develop lattice-mismatched GaInAsP as an alternative alloy to pure As-based alloys currently used in III–V multijunction solar cells. Increasing the alloy phosphorous and indium content while maintaining an optimal bandgap may allow high efficiency multijunction devices with increased radiation hardness. Here, 1.0-eV GaInAsP is developed and implemented into single and multijunction solar cell devices. The lattice-mismatched GaInAsP must be grown strain free, and the subcell thickness must be maintained below the thickness where surface-driven phase separation occurs. As observed in transmission electron microscopy and cathodoluminescence imaging, phase separation strengthens in the GaInAsP layer and leads to interfacial defect formation when the cell thickness is too great. We show single junction 1.0-eV $Ga_{0.5}In_{0.5}As_{0.7}P_{0.3}$ with excellent carrier collection and a bandgap-voltage offset of 0.40 V. This material quality approaches that of 1.0-eV $Ga_{0.7}In_{0.3}As$ used in inverted metamorphic multijunction devices, but has increased phosphorus content and consequently is expected to have a higher radiation resistance. We incorporate the 1.0-eV GaInAsP subcell into a 3-junction inverted metamorphic solar cell to test the performance of the subcell in a multijunction. No additional loss is observed upon integration into a multijunction cell: both the carrier collection and voltage of the GaInAsP subcell are unchanged from single junction devices. While further materials development and radiation testing is still required, these preliminary results indicate that lattice-mismatched GaInAsP can be effectively used in multijunction solar cells to replace radiation-soft materials.**

***Index Terms*—Gallium arsenide, photovoltaic cells, radiation hardening, III-V semiconductor materials.**

Manuscript received June 10, 2019; revised August 26, 2019; accepted October 8, 2019. Date of publication October 31, 2019; date of current version December 23, 2019. This work was supported in part by Northrop Grumman under the Space Solar Power Initiative, in part by The Aerospace Corporation, in part by the U.S. Department of Energy (DOE) under Contract No. DE-AC36-08GO28308 with Alliance for Sustainable Energy, LLC, the operator of the National Renewable Energy Laboratory, and California Institute of Technology under CRADA No. CRD-17-704, and in part by MRSEC Program of the NSF under Award No. DMR 1720256. The work of B. B. Haidet was supported by the National Science Foundation (NSF) Graduate Research Fellowship under Grant 1650114. *(Corresponding author: Ryan M. France.)*

R. M. France and H. L. Guthrey are with the National Renewable Energy Laboratory, Golden, CO 80401 USA (e-mail: ryan.france@nrel.gov; harvey.guthrey@nrel.gov).

P. Espinet-Gonzalez and H. A. Atwater are with the Applied Physics and Materials Science, California Institute of Technology, Pasadena, CA 91101 USA (e-mail: pespinet@caltech.edu; haa@caltech.edu).

B. B. Haidet and K. Mukherjee are with the Materials Department, University of California Santa Barbara, Santa Barbara, CA 93106 USA (e-mail: bbhaidet@ucsb.edu; kunalm@ucsb.edu).

D. Walker is with the The Aerospace Corporation, El Segundo, CA 90245 USA (e-mail: don.walker@aero.org).

Color versions of one or more of the figures in this article are available online at http://ieeexplore.ieee.org.

Digital Object Identifier 10.1109/JPHOTOV.2019.2947555

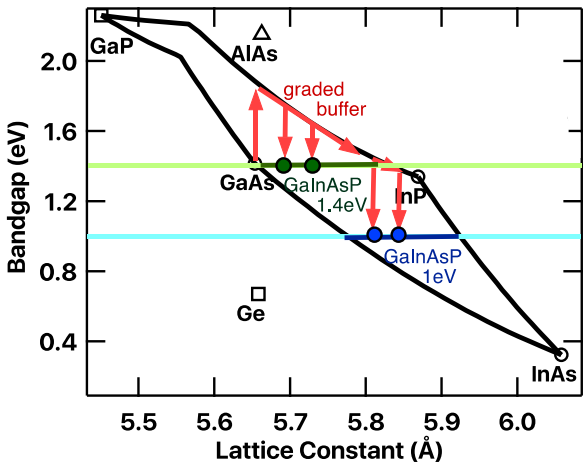

Fig. 1. Bandgap versus lattice constant of III–V alloys. The black lines are GaInAs, GaInP, GaAsP, and InAsP ternary tie lines, and the space between the tie lines are all potential quaternary GaInAsP alloys. Alloys with 1.4 and 1.0 eV are highlighted in dark green and blue, respectively, and are accessible using graded buffers on GaAs substrates. GaInAsP can replace 1.4-eV GaAs or 1.0-eV GaInAs alloys while retaining the same bandgap, potentially improving the radiation hardness of multijunction solar cells.

I. Introduction

MULTIJUNCTION solar cells for space applications demand tolerance to ionizing radiation from high energy particles. The tolerance to radiation damage varies with the semiconductor alloy, and therefore each subcell of a multijunction solar cell responds differently to irradiation. As-based subcells, such as the 1.4-eV GaAs and 1.0-eV GaInAs of inverted metamorphic multijunctions, are relatively radiation soft, while the GaInP subcell tends to be radiation hard, which has been theorized to be related to the high phosphorus and indium content [1]. Increasing the phosphorus content of the radiation-soft GaAs or GaInAs alloys while maintaining an optimal bandgap may allow high efficiency multijunction devices with increased radiation hardness.

Previous work has demonstrated lattice-matched 1.55-eV GaInAsP for space applications, showing good radiation tolerance [2] and 1.7-eV GaInAsP for excellent terrestrial solar cells [3], [4]. However, many of the key GaInAsP alloys are lattice-mismatched to GaAs or Ge substrates, including 1.4-eV and 1.0-eV materials. Fig. 1 shows the range of lattice-mismatched GaInAsP alloys that can replace 1.4-eV GaAs and 1.0-eV GaInAs subcells. Fig. 2 shows the specific compositions and

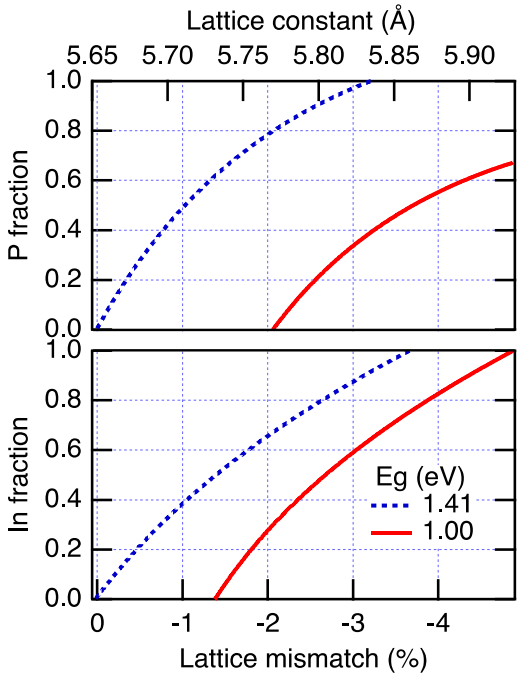

Fig. 2. GaInAsP alloy composition versus lattice mismatch to GaAs for a fixed bandgap of 1.41 eV (blue lines) and 1.00 eV (red lines). $Ga_{1-y}In_yAs_{1-x}P_x$ composition is plotted with the phosphorus fraction x in the top graph and the indium fraction y in the bottom graph. A wide range of GaInAsP alloys are accessible via lattice-mismatch to replace the 1.4 or 1.0 eV subcells of a multijunction solar cell.

lattice constants of 1.4-eV and 1.0-eV GaInAsP. As an example, $Ga_{0.6}In_{0.4}As_{0.5}P_{0.5}$ has 50% P-content and a similar bandgap to GaAs but is 1.1% lattice-mismatched to GaAs substrates [5]. Likewise, $Ga_{0.5}In_{0.5}As_{0.7}P_{0.3}$ has 30% P-content and a similar bandgap to the 1.0-eV GaInAs in inverted metamorphic multijunction devices, but is 2.8% lattice mismatched rather than 2.0% mismatched. As seen in Fig. 2, increasing the lattice mismatch accesses alloys with increasing phosphorus contents but equivalent bandgap [5].

While lattice-mismatched GaInAsP may increase radiation hardness, it has several challenges that may reduce performance and limit its use, thus requiring investigation. GaInAsP contains a miscibility gap and therefore, is prone to spinodal decomposition [6], [7]. Composition fluctuations can manifest at the III–V growth surface, and may be aggravated by the nonuniform, undulating (crosshatched) surface of a metamorphic buffer. In addition, lattice-mismatched material necessarily contains dislocations, which can alter growth parameters and degrade solar cell performance, and the buffers required for these GaInAsP alloys are more mismatched than for their As-based alloy counterparts.

Here, we develop lattice-mismatched 1.0-eV $Ga_{0.5}In_{0.5}As_{0.7}P_{0.3}$ and implement the material within single and multijunction solar cell devices. This GaInAsP alloy has a relatively high lattice mismatch, 2.8%, and therefore, gauges the feasibility of the immiscible quaternary on a crosshatched metamorphic template. GaInP graded buffers with the appropriate lattice mismatch are developed and used to study the growth of lattice mismatched GaInAsP, which is investigated using *in situ* and *ex situ* material characterizations. The ultimate impact of the lattice mismatch on overall solar cell performance is directly measured using device characteristics.

II. Experimental

All material was grown by atmospheric-pressure metalorganic vapor phase epitaxy on (001) GaAs substrates miscut 2° toward (111)B. The mixed anion incorporation was initially studied using a GaAsP buffer grown on GaP substrates, and all other growths were on GaAs substrates. 1.0-eV GaInAsP and GaInAs single junction solar cells were grown inverted, first with an n-type GaInNAs:Se contact layer, followed by an n-type GaInP:Si graded buffer (growth conditions and structure described elsewhere [8], [9]) and 1 μm of strain-free n-GaInP. Because of the higher lattice mismatch, the thickness of the graded buffer for the 1.0-eV GaInAsP solar cell was 1.1 μm greater than the 1.0-eV GaInAs solar cell. Then, p-type GaInAsP:Zn or GaInAs:Zn, doped 2×10^{17} cm^{-3}, was then grown, forming a heterojunction with the n-GaInP. The GaInAsP was grown at 650 °C with a V/III ratio of 250, and at a growth rate of 6 μm/hr. Phosphine and arsine were used as group V precursors at a phosphine/arsine ratio of 11.5 in the strain-free devices, and triethylgallium and trimethylindium are used as group III precursors. 300 nm of p-type GaInP:Zn was then deposited as a back passivation layer followed by a 100 nm p+ GaInAsP:Zn contact layer.

Triple-junction inverted metamorphic (3J IMM) devices were grown using the same structure described previously [10], but with few exceptions: the GaAs subcell was 2.5-μm thick, and the metamorphic subcell consists of 1.0-eV GaInAsP instead of GaInAs. The structure of the GaInAsP subcell in the 3J IMM device was identical to the single junction test structure.

In situ measurements were performed using a multibeam optical stress sensor, which reflects an array of 662-nm laser light off the sample throughout growth. The *in situ* stress was determined from the curvature of the GaInAsP during growth, which was calculated from the amount of deflection, and the roughness was qualitatively gauged from the intensity of the reflected beams.

Samples were processed using an inverted procedure [10]. Planar Au was first deposited onto the p+ GaInAsP contact layer, and then the sample was inverted and bonded onto a Si handle using epoxy and the GaAs substrate was removed. Front NiAu grids were then deposited with 150–225 μm pitch, 0.1-cm^2 devices were isolated, and the GaInNAs contact layer was removed.

Quantum efficiency (QE) was measured on a custom system using LEDs for optical bias, and the data were corrected for luminescent coupling. Bandgaps were determined from the external QE using methods described previously [11]. The specular reflection was measured simultaneously to the external QE and used to determine the internal QE. 1-sun IV data under the AM0 spectrum (1366 W/m^2, 25 °C) were measured on an adjustable-sun simulator using spectral correction factors and LEDs to tune the spectrum. Electroluminescence was measured on a custom tool using a calibrated fiber optic and spectroradiometer, and

the subcell IV curves were determined using methods described previously [11].

Scanning transmission electron microscopy (STEM) was performed on an unprocessed portion of the sample using an FEI Talos microscope operating at 200 kV. An FEI Helios NanoLab dual-beam microscope was used to lift out a thin cross-sectional foil normal to the [−110] direction. The final sample polish utilized a 2-kv Ga-ion beam. Bright field (BF STEM) images were recorded using a 17-mrad aperture after tilting the sample to excite the strain-sensitive $g = 220$ diffraction.

Cathodoluminescence (CL) imaging was performed on an unprocessed piece of the sample in a JEOL JSM-7600 FESEM equipped with a Horiba CLUE CL system. Images were acquired at 25 °C using a 15-kV accelerating voltage and ∼4-nA electron beam current. Emission from the sample was collected using a parabolic mirror and an InGaAs detector. Four 60 × 60 μm scans were collected per sample and integrated intensity images were created to determine the defect density (averaged over all images).

All GaInAsP compositions were determined from the bandgap and lattice constant using [5], which was also used for the calculations in Figs. 1 and 2.

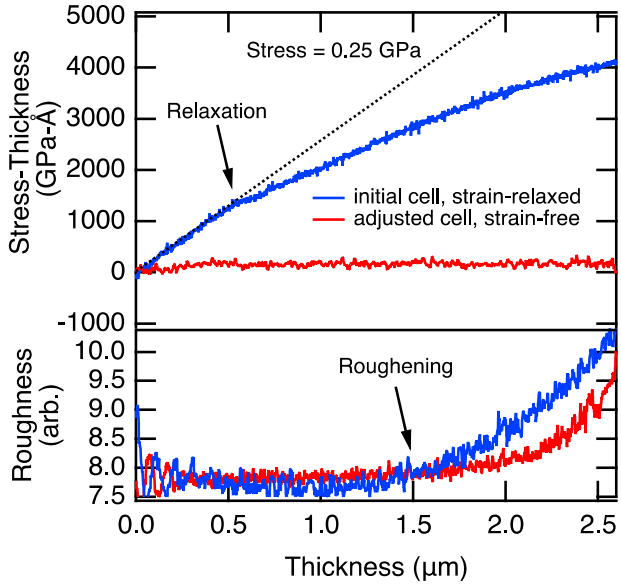

Fig. 3. *In situ* curvature analyses of lattice-mismatched GaInAsP. Stress thickness (top) shows that initial devices strain relaxed, and roughness (bottom) is observed after 1.5 μm of GaInAsP growth, potentially because of phase separation.

III. Results

A. Lattice-Mismatched GaInAsP: Epitaxy and Device Results

1.0-eV GaInAsP composition tuning was performed by first calibrating the mixed anion incorporation efficiency using a GaAsP graded buffer grown on GaP (not shown). Then, GaInP:Si graded buffers were developed with the in-plane lattice demanded by a 1.0-eV GaInAsP material with approximately 30% P-content as determined by [5]. Initial group V gas flows of the GaInAsP were determined from the GaAsP calibration curve.

Initial GaInAsP was strained and the bandgap was lower than targeted. The average stress for the first 0.5 μm of growth, determined from the slope of the stress-thickness product (blue line in Fig. 3), is 0.25 GPa, after which strain relaxation is observed, indicated by a change in the slope of the stress thickness. Based on the stress and the bandgap (shown later), adjustments to the group V flows were made to create strain free, 2.6-μm thick, 1.0-eV material (red line in Fig. 3) with a nominal composition of $Ga_{0.5}In_{0.5}As_{0.7}P_{0.3}$.

Both strain-relaxed and strain-free GaInAsP materials begin significantly roughening at thicknesses greater than 1.5 μm, observed using the laser power of the *in situ* wafer curvature tool, and shown in Fig. 3. Roughness during growth of lattice-matched GaInAsP has previously been correlated with surface-driven phase separation, where the top-most material begins to degrade after a certain thickness [12].

STEM is performed on the thick, strain-free sample to observe any internal phase separation, shown in Fig. 4. The top of Fig. 4 shows a large-area view of the entire structure. Within the field of view, no dislocations penetrate from the graded buffer into the GaInAsP, indicating good dislocation confinement within the buffer. However, composition modulation is visible in the GaInAsP, as indicated by the vertical contrast. The contrast strengthens toward the top of the GaInAsP layer, indicating increasing compositional fluctuations throughout the growth of the layer. A closer view of the GaInAsP-GaInP BSF interface is shown in the bottom of Fig. 4. Interfacial defects form at points where composition fluctuations are greatest. The defects appear to propagate on (111) planes and are likely stacking faults that originate at the interface. Multiple defects are observed within the STEM field of view, indicating a high density in the sample.

Phase separation in GaInAsP has previously been shown to be surface driven and can be modified using growth conditions, such as growth temperature [12], [13]. Here, using identical GaInP graded buffers, we simply thin the subsequent GaInAsP to 1 μm, which is prior to the roughening observed in *in situ* measurements, and prior to the strong contrast shown in STEM.

Cathodoluminescence images of 1.0-eV lattice-mismatched GaInAsP solar cell structures with strain-free 2.6 and 1.0 μm GaInAsP absorbing layer thickness are shown in Fig. 5. The 2.6-μm GaInAsP is highly defective, while the 1.0-μm GaInAsP has a dark spot density of 1×10^6 cm^{-2} (averaged from 0.014 mm^2). Because there is no difference between the GaInP graded buffers, the residual threading dislocation density from the buffer should be identical between the samples. Indeed, 1×10^6 cm^{-2} residual threading density has previously been shown for GaInP buffers in this lattice-constant range [14], [15], and therefore, is expected. The additional dark spots in the 2.6-μm sample are likely from the defects generated at the GaInAsP-GaInP interface, shown in the bottom of Fig. 4.

The external QE, internal QE, and IV data of all single-junction GaInAsP cell results are shown in Fig. 6, and compared with a high-performance 1.0-eV GaInAs cell. In order to compare the bandgap-voltage offsets (Wocs) between samples, the current density in the *JV* data for all samples is normalized

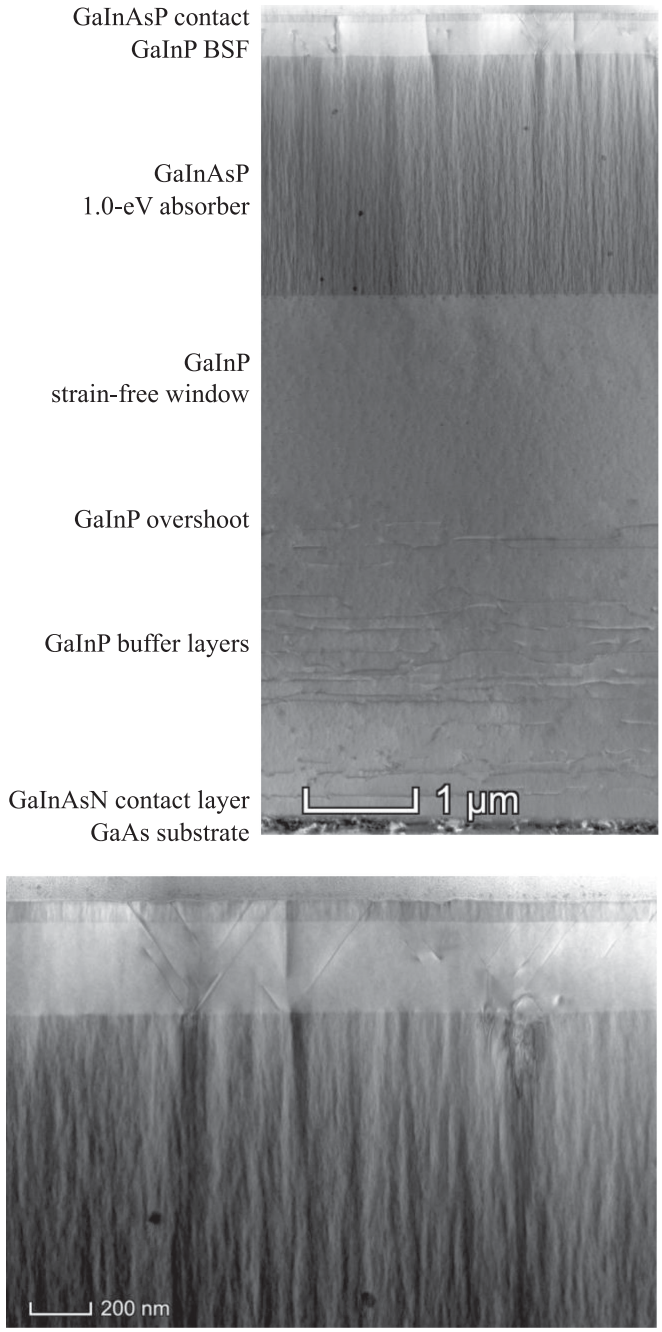

Fig. 4. STEM imaging of thick, lattice-mismatched GaInAsP on a metamorphic GaInP graded buffer. (Top) View of full structure, showing dislocation confinement within the graded buffer, but compositional modulation in the GaInAsP. (Bottom) Defects form at the interface between the GaInP BSF and GaInAsP at regions with greatest compositional fluctuations.

to 15 mA/cm^2, the expected operating current in a 3J IMM. The thick, unoptimized, strain-relaxed GaInAsP (blue lines in Fig. 6) performs poorly, as anticipated, with a large QE loss and low voltage. Proper strain-balancing a 2.6-μm thick GaInAsP cell improves performance (red lines in Fig. 6), but the phase separation and associated defects still limit performance. Thinning the device to 1.0 μm in order to avoid severe phase separation improves QE and voltage (green lines in Fig. 6). The

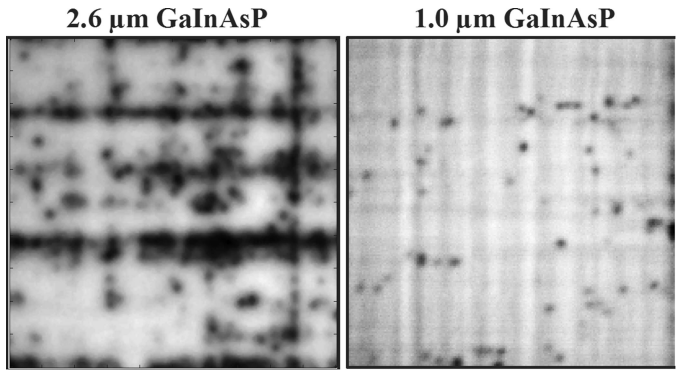

Fig. 5. 60 × 60 μm cathodoluminescence images of lattice-mismatched 1.0-eV GaInAsP solar cell structures with (left) 2.6 μm and (right) 1.0 μm GaInAsP absorber thickness.

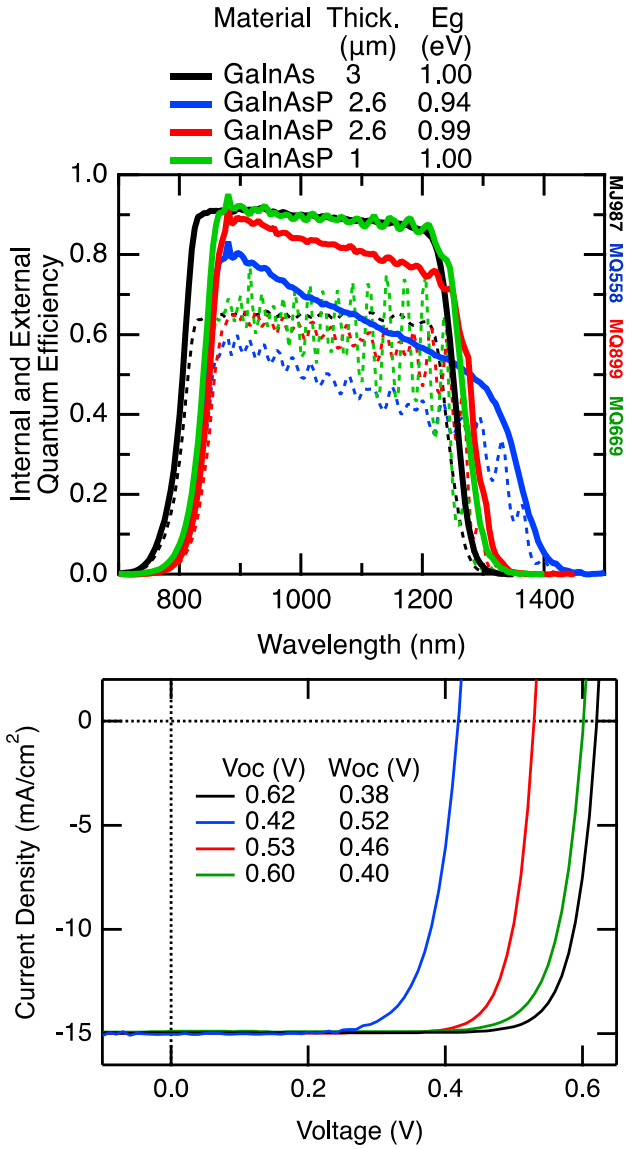

Fig. 6. (Top) Internal (solid lines) and external (dashed lines) QE, and (bottom) J–V results normalized to 15 mA/cm^2 for 1.0-eV GaInAs (black) and 1.0-eV GaInAsP solar cells. Blue data are from GaInAsP that showed strain relaxation and red data are from GaInAsP that showed signs of phase separation (see Fig. 2). High performance GaInAsP was achieved through proper strain balancing and avoiding defects associated with phase separation (green data).

1.0 μm thick GaInAsP cell is optically thin compared with the 3.0 μm thick GaInAs cell, as can be seen in the external QE. However, the internal QE gauges the collection efficiency for light that is absorbed, and is high for the 1.0 μm thick GaInAsP cell, indicating good material quality. The cell improvement upon thinning further supports the finding that phase separation strengthens throughout the layer and leads to harmful interfacial defect formation.

The 1-μm-thick 1-eV GaInAsP device performs very well, having a bandgap-voltage offset Woc = 0.40 at Jsc = 15 mA/cm^2, only 20 mV higher than high-performance lattice-mismatched 1.0-eV GaInAs. The voltage loss could be related to a small difference in threading dislocation density, or it could be related to other material differences between GaInAsP and GaInAs, such as the composition fluctuations observed in TEM. However, these initial results are very promising, and suggest that GaInAsP can be used in a multijunction device without major losses as long as phase separation is controlled.

Here, we control phase separation in lattice-mismatched GaInAsP simply by limiting the subcell thickness to a point before the onset of strong phase separation. Thin subcells are sometimes desirable in order to improve radiation hardness [16], and it is important to consider both the impact of subcell thickness on radiation hardness in addition to the impact related to alloy composition. Although thin GaInAsP may be beneficial for radiation hardness, high-quality optically thick GaInAsP is required for full absorption of the spectrum without a back reflector. The capability to create high-quality optically thick material also enables a less complex tradeoff between current collection and radiation hardness as the thickness is changed. Further work is necessary to limit surface-driven phase separation in lattice-mismatched, optically-thick, high-quality GaInAsP, which was previously demonstrated on lattice-matched GaInAsP by modifying growth conditions [12]. However, the QE in these GaInAsP devices is high although the subcell is only 1-μm thick because there is an Au back reflector behind the bottom cells of IMM devices, making this device appropriate to test in a 3J IMM to determine if there are any issues limiting the use of lattice-mismatched GaInAsP in a multijunction device.

B. 3-Junction IMM Using GaInAsP

The 1.0-eV GaInAsP subcell developed above is implemented into a 3J IMM, replacing the 1.0-eV GaInAs subcell, to test the subcell performance in a multijunction and investigate any potential integration issues. The cell is not optimized for space use, and has a high shadow factor and no antireflective coating (ARC). However, the cell performs well, and results are shown in Fig. 7. Although the GaInAsP is not optically thick, the EQE and IQE in the GaInAsP subcell are good: no long-wavelength loss is observed and the height of the QE matches the height of the GaAs subcell. No significant QE loss is observed between the GaAs subcell and the GaInAsP subcell, showing that the GaInP buffer is still sufficiently transparent despite the buffer containing more indium than the buffer in standard 3J IMM devices. Even though thin, the GaInAsP bottom cell has 11% excess current compared with the GaInP top cell. Although not shown here, fine tuning

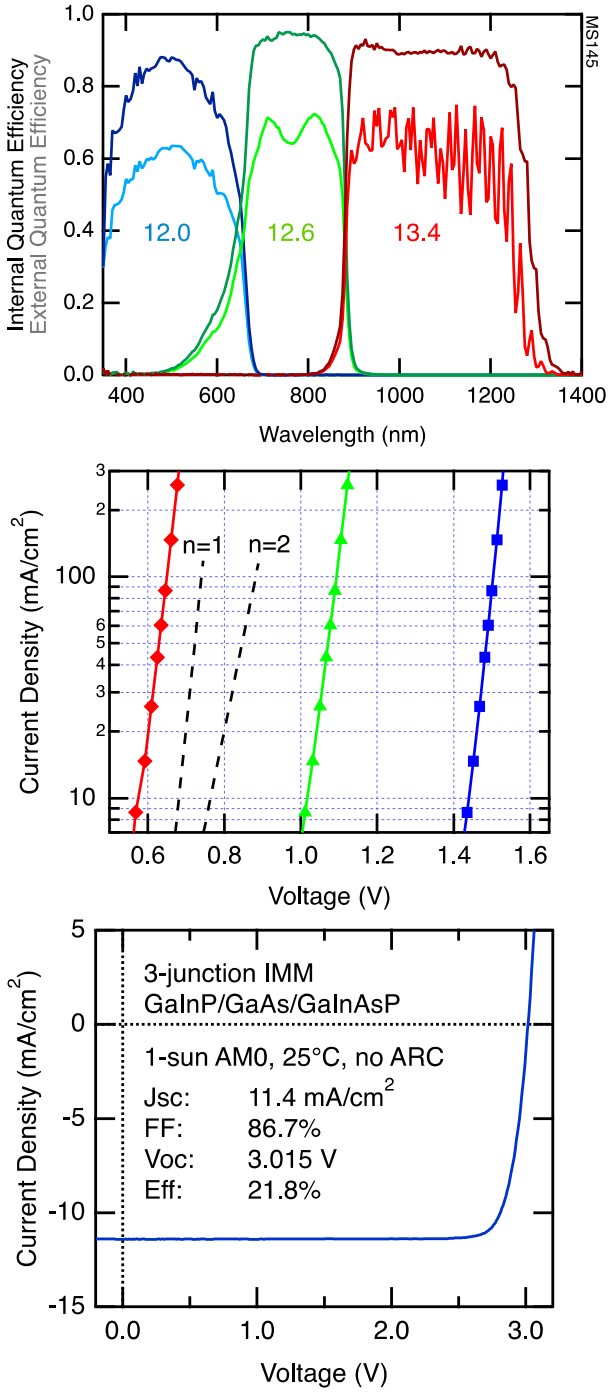

Fig. 7. (Top) Internal and external quantum efficiency and integrated currents under the AM0 spectrum of a 3J IMM with a $Ga_{0.5}In_{0.5}As_{0.7}P_{0.3}$ bottom subcell. (Middle) Subcell dark *JV* curves, calculated using electroluminescence. Junctions 1, 2, and 3 characteristics are colored blue, green, and red, respectively. The dashed black lines show the slopes of ideal diodes with $n = 1$ and $n = 2$ for reference. (Bottom) 1-sun *J–V* curve taken under the AM0 spectrum at 25 °C with 1366-W/m^2 irradiance.

the subcell photocurrent should be possible by adjusting the composition and bandgap of the GaInAsP.

The subcell dark-current voltages are calculated from electroluminescence measurements, and shown in the middle of Fig. 7. The first, second, and third subcells have voltages of

1.45, 1.03, and 0.59 V at 15 mA/cm^2, respectively. From the EQE, the bandgap of the GaInAsP subcell is 0.99 eV, meaning that the subcell Woc in a multijunction is unchanged from its single-junction counterpart: 0.40 V. The slope of the DIV is very close to n = 1 ideality behavior. The *J–V* characteristics are shown in the bottom of Fig. 7. High Voc and fill factor are achieved, and nearing the performance of highly optimized GaInP/GaAs/GaInAs 3-junction devices [10], [17]. The Jsc is low because of the lack of an ARC as well as imperfect photocurrent distribution. Overall, the device performs very well and we determine that there are no issues with integrating 1.0-eV GaInAsP into a multijunction device.

IV. Conclusion

Lattice-mismatched GaInAsP was developed as an alternative to As-based subcells in multijunction devices. Using lattice-mismatched GaInAsP accesses alloys with equivalent bandgap to GaAs or GaInAs, but with higher phosphorus and indium content, which may improve radiation hardness. Single-junction 1.0-eV $Ga_{0.5}In_{0.5}As_{0.7}P_{0.3}$ solar cells with 2.8% lattice-mismatch to GaAs substrates are grown on GaInP graded buffers. STEM and CL imaging showed that phase separation exists in lattice-mismatched GaInAsP, and strengthens throughout the layer, eventually leading to defect formation at the interface with the subsequent GaInP passivation layer. Excellent voltage Woc = 0.40 V, and collection efficiency in single-junction 1.0-eV GaInAsP subcells are shown by controlling strain and limiting the thickness to 1.0 μm in order to avoid severe phase separation and defect formation, showing that good performance is possible if phase separation is controlled. The thin GaInAsP subcell is incorporated into a 3J IMM with no apparent integration issues related to the GaInAsP alloy. Although thin devices are sometimes desirable for radiation hardness, further work is needed in order to limit phase separation in optically thick GaInAsP. Further development and radiation testing is ongoing. However, based on these initial results, lattice-mismatched GaInAsP is a promising alternative to radiation-soft subcell alloys.

Acknowledgment

This work was authored by the National Renewable Energy Laboratory, operated by Alliance for Sustainable Energy, LLC, for the U.S. Department of Energy (DOE). The views expressed herein do not necessarily represent the views of the DOE or the U.S. Government. The U.S. Government retains and the publisher, by accepting the article for publication, acknowledges that the U.S. Government retains a nonexclusive, paid-up, irrevocable, worldwide license to publish or reproduce the published form of this work, or allow others to do so, for U.S. Government purposes. The authors thank Waldo Olavarría and Michelle Young for cell fabrication. Transmission electron microscopy was performed at the UCSB MRL Shared Experimental Facilities, which are supported by the MRSEC Program of the National Science Foundation (NSF); a member of the NSF-funded Materials Research Facilities Network.

References

[1] M. Yamaguchi, "Radiation-resistant solar cells for space use," *Sol. Energ Mater. Sol. Cells*, vol. 68, pp. 31–53, 2001.

[2] P. R. Sharps *et al.*, "Development of 20% efficient GaInAsP solar cells," in *Proc. 23rd IEEE Photovolt. Specialists Conf.*, 1993, pp. 633–638.

[3] N. Jain *et al.*, "High-efficiency inverted metamorphic 1.7/1.1 eV GaInAsP/GaInAs dual-junction solar cells," *Appl. Phys. Lett.*, vol. 112, 2018, Art. no. 053905.

[4] N. Jain, J. F. Geisz, R. M. France, A. G. Norman, and M. A. Steiner, "Enhanced current collection in 1.7 eV GaInAsP solar cells grown on GaAs by metalorganic vapor phase epitaxy," *J. Photovolt.*, vol. 7, pp. 927–933, 2017.

[5] R. L. Moon, G. A. Antypas, and L. W. James, "Bandgap and lattice constant of GaInAsP as a function of alloy composition," *J. Electron. Mater.*, vol. 3, pp. 635–644, 1974.

[6] A. G. Norman and G. R. Booker, "Transmission electron microscope and transmission electron diffraction observations of alloy clustering in liquid-phase epitaxial (001) GaInAsP layers," *J. Appl. Phys.*, vol. 57, pp. 4715–4720, 1985.

[7] K. Onabe, "Calculation of miscibility gap in quaternary InGaPAs with strictly regular solution approximation," *Jpn. J. Appl. Phys.*, vol. 21, pp. 797–798, 1982.

[8] R. M. France *et al.*, "Reduction of crosshatch roughness and threading dislocation density in metamorphic GaInP buffers and GaInAs solar cells," *J. Appl. Phys.*, vol. 111, pp. 103528–103528-7, 2012.

[9] R. M. France *et al.*, "Lattice-mismatched 0.7-eV GaInAs solar cells grown on GaAs using GaInP compositionally graded buffers," *J. Photovolt.*, vol. 4, pp. 190–195, 2013.

[10] J. F. Geisz *et al.*, "High-efficiency GaInP/GaAs/InGaAs triple-junction solar cells grown inverted with a metamorphic bottom junction," *Appl. Phys. Lett.*, vol. 91, 2007, Art. no. 023502.

[11] J. F. Geisz *et al.*, "Generalized optoelectronic model of series-connected multijunction solar cells," *J. Photovolt.*, vol. 5, pp. 1827–1839, 2015.

[12] R. Oshima, R. M. France, J. F. Geisz, A. G. Norman, and M. A. Steiner, "Growth of lattice-matched GaInAsP grown on vicinal GaAs(001) substrates within the miscibility gap for solar cells," *J. Cryst. Growth*, vol. 458, pp. 1–7, 2016.

[13] K. Mukherjee, A. G. Norman, A. J. Akey, T. Buonassisi, and E. A. Fitzgerald, "Spontaneous lateral phase separation of AlInP during thin film growth and its effect on luminescence," *J. Appl. Phys.*, vol. 118, 2015, Art. no. 115306.

[14] I. Garcia *et al.*, "Metamorphic III-V solar cells: Recent progress and potential," *J. Photovolt.*, vol. 6, pp. 366–373, 2015.

[15] R. M. France, F. Dimroth, T. J. Grassman, and R. R. King, "Metamorphic epitaxy for multijunction solar cells," *MRS Bull.*, vol. 41, pp. 202–209, 2016.

[16] J. G. J. Adams *et al.*, "Improved radiation resistance of epitaxial lift-off inverted metamorphic solar cells," in *Proc. IEEE 39th Photovolt. Specialists Conf.*, Tampa, FL, USA, 2013, pp. 3229–3232.

[17] R. M. France *et al.*, "Pushing inverted metamorphic multijunction solar cells towards higher efficiency at realistic operating conditions," *J. Photovolt.*, vol. 3, pp. 893–898, 2013.